HAIT Journal of Science and Engineering B, Volume 2, Issues 3-4, pp. 365-385

Six-phase synchronous generator-rectifier parametric average value modeling considering operational modes

Juri Jatskevich[1,*] and Steven D. Pekarek[2]

[1] *Department of Electrical and Computer Engineering, University of British Columbia, Vancouver, BC V6T1Z4, Canada*
[2] *Department of Electrical and Computer Engineering, Purdue University, West Lafayette, IN 47907, USA*
[*] *Corresponding author: jurij@ece.ubc.ca*

Received 1 March 2005, accepted 10 July 2005

Abstract

In a wide range of applications, a synchronous generator is directly connected to a converter which then feeds into a dc system. Derivation of accurate dynamic average value models (AVM) of a high-pulse-count generator-rectifier system depends upon operational modes. In this paper, a parametric approach to construct an AVM is developed for a system comprised of a 240Hz 6-phase synchronous generator-rectifier and an interphase transformer. The system exhibits several distinct operational modes for which the analytical derivation of the AVM is nearly intractable. The proposed method of generating the AVM avoids extensive analytical derivations – although it does require an initial simulation of a detailed switched model of the system from which the rectifier/dc-link dynamics is found by using numerical averaging. The results obtained from the developed AVMs are compared against detailed simulations, and for each considered mode an excellent agreement is demonstrated.

Keywords: Six phase synchronous generator, rectifier, operational mode, average value model, output impedance.

1 Introduction

Many of the methods used to investigate the stability and design/tune controllers for systems with electrical machines and power electronics rely upon an impedance-based approach [1,2]. A traditional method of extracting the impedance of non-linear power electronic-based systems utilizes frequency sweep [3]. However, an effective procedure, determining the impedance over a wide range of frequencies is very time consuming, particularly when using a computationally intensive detailed model that includes switching and obtaining many data points at very low frequencies. In addition, for some system-level studies with a large number of power-electronic modules, the details of switching in an individual module (source or load) may not be as important as the overall dynamic interaction at lower frequencies. For these studies, modeling the entire system in detail will result in significant simulation times.

These challenges have led to the development of the so-called average-value models wherein the effects of fast switching are neglected or "averaged" with respect to the prototypical switching interval, and the respective state variables are constant in the steady-state. Although the resulting nonlinear models only approximate the slower dynamics of the original systems, they are continuous and therefore can be linearized around a desired operating point. Thereafter, obtaining a local transfer function becomes a straightforward and almost instantaneous procedure. Many simulation programs offer automatic linearization and subsequent state-space and/or frequency-domain analysis tools, for example [4].

The analytical derivation of average-value models for synchronous machine-converter systems is difficult. Initial steps in this direction for a fixed reactance behind a voltage source can be found in [5,6]. Reduced order models with neglected stator dynamics have been presented in [7,8]. A dynamic average model has been derived in [9], wherein a very good match in time- and in frequency-domains with the detailed simulation is reported. For the inductor-less case, the model has been developed in [10]. The analytical development of all of these models is based upon a single switching pattern (conduction and commutation intervals) and therefore is valid only for a single operating mode. An approach similar to [5] has been also used recently with synchronous generators in [11], wherein the parameters of the rectifier average-value model are obtained from a detailed simulation. However, in [11], in addition to requiring a non-proper generator model with voltages as the outputs, the rectifier model parameters are not dependent on operating condition.

A parametric averaging of a rectifier circuit for a three phase synchronous machine-rectifier-system has been set forth in [12], wherein the functions defining the relationship between the averaged dc-link variables and the generator currents and voltages viewed in the rotor reference frame were extracted numerically for a specified range of the loading condition. The method presented in this paper extends the work [12] to several configurations of a six phase system with an interphase transformer. Moreover, since for the purpose of this paper only the small-signal characteristics are considered, the functions defining the relationship between the averaged dc-link variables and the generator currents and voltages viewed in the synchronous reference frame are implemented using linear approximations, which significantly simplifies the model development and results in a very fast procedure for impedance characterization.

2 Generator rectifier system

2.1 System description

The system considered herein is comprised of a six-phase 210kW 240Hz special purpose synchronous generator designed for naval applications [13]. The overall system is depicted in Fig. 1. In the given generator, the stator windings are grouped as two sets of Y-connected 3-phase windings that are geometrically displaced from each other by 60 electrical degrees. The corresponding neutral points can be isolated or connected to each other by the switch S. As shown in Fig. 1, each set of windings is connected to an uncontrolled rectifier. The rectifiers have a common negative rail and their positive rails are connected to the output capacitor C_f through the interface transformer that is supposed to improve the current balance as well as reduce ripple. The generator model also includes a field winding fd and a damper winding kq and kd in the q- and d-axes of the rotor, respectively. This system has been previously modeled [13–15] and for consistency the parameters are summarized in Table 1.

The possibility of connecting/disconnecting the generator neutrals, including/excluding the interphase transformer, etc., results in different operational modes under the same load. Moreover, these operational modes are difficult to analyze analytically which represent a big challenge for constructing the appropriate average-value model. As will be shown later, the operational modes also affect the output impedance of the system. In this paper, the system depicted in Fig. 1 is considered with four variations:

1. without transformer and neutrals disconnected,
2. without transformer and neutrals connected,
3. with transformer and neutrals disconnected,
4. with transformer and neutrals connected.

Various modes of this system have been analyzed and compared with the hardware measurements in [15]. Herein, the system of Fig. 1 is viewed as a source and its output impedance is determined using the averaged-value model developed using the parametric approach.

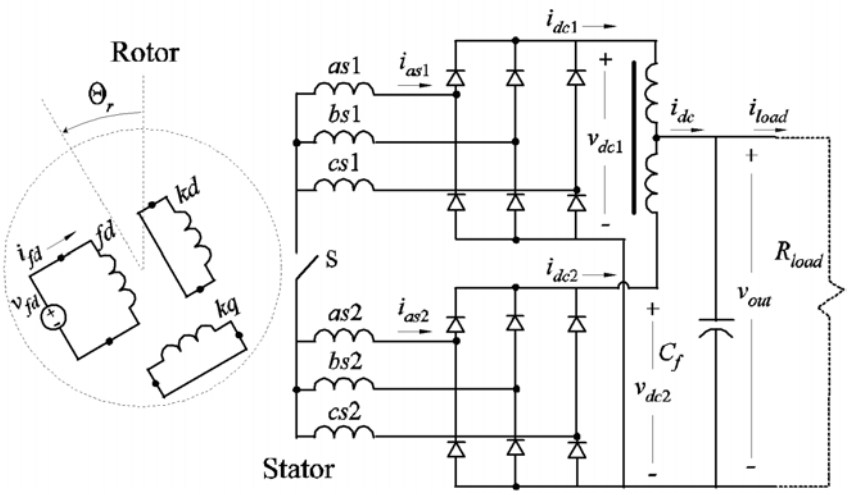

Figure 1: Six-phase generator-rectifier system.

2.2 Detailed model

When modeling power electronic-machine systems in detail, it is often more convenient to represent the electrical machine stator network in terms of physical *abc* variables, rather than transformed $q-d$ variables. Based on physical variables, an electrical machine can be represented using simple circuit elements: voltage sources, resistors, and coupled inductors. The stator windings are magnetically coupled with the rotor and each other. Such coupled-circuit machine model is also sometimes referred to as the phase-domain model, and has been used many times with the state variable approach, for example in [16], as well as the nodal analysis approach [17].

The synchronous generator can be modeled in a so-called voltage-behind-reactance (VBR) form [18] where the rotor state equations are expressed in terms of transformed $q-d$ variables, and the stator coupled-inductor network is in terms of physical *abc* variables. As shown in [18], such model is absolutely equivalent to the coupled-circuit model, as well as the full-order Park's model. The resulted implementation is depicted in Fig. 2. The advantage of the model depicted in Fig. 2 is that the stator network is directly interconnected with the converter network and the rest of the electrical system. In addition, the system of Fig. 2 can also be modeled with the so-called dynamic saliency neglected [19]. This modeling technique results in a constant stator inductance matrix, which provides a significant computational advantage, and is equivalent to the Park's representation [20,21] over a wide range of frequencies. For the six phase case, the relevant equations can be found in [18,19,22] and, therefore, are not repeated here.

Branch(s)/Parameter	Symbol	Value
Base frequency	ω_b	1507 r/s
13-18, Stator winding resistance	r_s	0.114Ω
13-18, Stator winding leakage	L_{ls}	0.135mH
Magnetizing inductance q-axis	L_{mq}	1.60mH
Damper winding q-axis resistance	r_{kq}	0.110Ω
Damper winding q-axis leakage	L_{lkq}	0.06mH
Magnetizing inductance d-axis	L_{md}	1.82mH
Damper wind. d-axis resistance	r_{kd}	0.118Ω
Damper winding d-axis leakage	L_{lkd}	0.650mH
Coupling of leakage fluxes	L_{lm}	0.045mH
Field winding d-axis resistance	r_{fd}	0.015Ω
Field winding d-axis leakage	L_{lfd}	0.255mH
Interphase trans. winding resistance	r_{tr}	0.05Ω
Interphase trans. mutual inductance	$L_{m,tr}$	1.0mH
Interphase trans. leakage inductance	L_{ltr}	0.25mH
Output capacitor	C_f	2μF
Load resistance	r_{load}	12Ω

Table 1: System parameters.

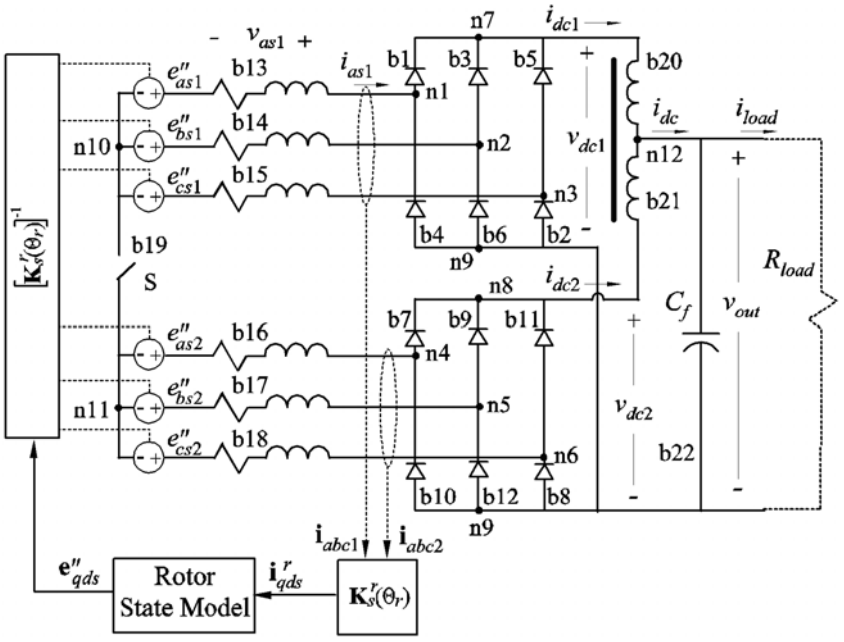

Figure 2: Voltage-behind-reactance implementation of the six-phase generator-rectifier system.

The stator windings together with the rectifier represent a switched network. For each topological instance of the system depicted in Fig. 2 there exists a corresponding state equation. However, due to the large number of phases and the rectifier switching, analytically establishing a state model for all potential topologies is very challenging. To overcome this challenge, an algorithm for generating the state equations has been developed in [15,16,23] and [24]. Utilizing this approach, a circuit is defined by a branch list composed of statements such as

L_branch(bn, pn, nn, r, L, e, Iic);

which defines an inductive branch, for example. Here, **bn** is the branch number; **pn** and **nn** are the positive and negative nodes; **r**, **L**, and **e** are the branch series resistance, inductance, and the voltage source; and **Iic** is the initial inductor current, respectively. A mutual inductance can be specified using the statement

L_mutual(b1, b2, Lm);

where **b1** and **b2** are the inductive branch numbers and **Lm** is the respective mutual inductance. Other circuit branches may be defined using similar

syntax. For consistency, the branch numbering is also shown in Fig. 2. As the circuit switches, a state equation is automatically generated and updated for each new topology.

The reference frame transformation $\mathbf{K}_s^r(\theta_r)$ shown in Fig. 2 is obtained by extending the standard Park's transformation

$$\mathbf{K}_s^{3\phi}(\theta) = \frac{2}{3}\begin{bmatrix} \cos\theta & \cos(\theta - 2\pi/3) & \cos(\theta + 2\pi/3) \\ \sin\theta & \sin(\theta - 2\pi/3) & \sin(\theta + 2\pi/3) \\ 1/2 & 1/2 & 1/2 \end{bmatrix} \tag{1}$$

to the six phase system considered herein as

$$\mathbf{f}_{qd0} = \frac{1}{2}\begin{bmatrix} \mathbf{K}_s^{3\phi}(\theta_r) & \mathbf{K}_s^{3\phi}(\theta_r - \pi/3) \end{bmatrix} \cdot \begin{bmatrix} \mathbf{f}_{abc1} \\ \mathbf{f}_{abc2} \end{bmatrix} = \mathbf{K}_s^r(\theta_r) \cdot \begin{bmatrix} \mathbf{f}_{abc1} \\ \mathbf{f}_{abc2} \end{bmatrix} \tag{2}$$

where $\mathbf{f}_{qd0} = \begin{bmatrix} f_q & f_d & f_0 \end{bmatrix}^T$, and the two three-phase sets $\mathbf{f}_{abc1} = \begin{bmatrix} f_{a1} & f_{b1} & f_{c1} \end{bmatrix}^T$ and $\mathbf{f}_{abc2} = \begin{bmatrix} f_{a2} & f_{b2} & f_{c2} \end{bmatrix}^T$ are assumed to be shifted by $\pi/3$. Here f may represent current, voltage, or flux.

The entire system was implemented in Matlab/Simulink [4]. The standard Simulink library blocks were used to implement the rotor state model and the reference frame transformations. The stator network together with the rectifiers, the interphase transformer, and the load, were implemented using the automated state-variable-based toolbox described in [23], wherein the appropriate switching logic is implemented to model the rectifier circuit in valve-by-valve detail assuming idealized on/off switching characteristics. As shown in Fig. 2, the generator neutrals can be connected/disconnected using the switch S branch 19.

3 Parametric average value modeling

The dynamic average-value model of the rectifier circuit relies upon establishing a relationship between the dc-link variables on the one side and the ac variables transferred to a suitable reference frame on the other side. In particular, with respect to the transformation (2), it is convenient to consider a synchronous reference frame in which the averaged d-axis component of the rectifier input ac voltage is identically zero. The resulting synchronous reference frame and relationship of the corresponding variables is shown in Fig. 3, wherein the transformation angle θ_e is selected to ensure that $\bar{v}_{ds}^e = 0$, which implies that the q^e-axis is synchronized with the peak of the phase

$a1$ rectifier input ($abc1$) voltages. Here, the superscripts "e" and "r" denote the synchronous and rotor reference frames, respectively; whereas the bar symbol denotes the so-called fast average

$$\bar{f} = \frac{1}{T_{sw}} \int_{t-T_{sw}}^{t} f(t)\, dt \tag{3}$$

evaluated over a prototypical switching interval T_{sw}. For the given generator with its two sets of windings shifted by 60 degrees and 240Hz base frequency, the complete prototypical switching interval is $T_{sw} = 1/1440$sec. The averaged generator voltages expressed in the rotor reference frame are $\bar{v}^r_{qs}$ and $\bar{v}^r_{ds}$. Based on Fig. 3, the relationship between the voltages in the rotor and synchronous reference frames is

$$\begin{bmatrix} v^e_{qs} \\ 0 \end{bmatrix} = \begin{bmatrix} \cos(\delta) & \sin(\delta) \\ -\sin(\delta) & \cos(\delta) \end{bmatrix} \cdot \begin{bmatrix} v^r_{qs} \\ v^e_{ds} \end{bmatrix}. \tag{4}$$

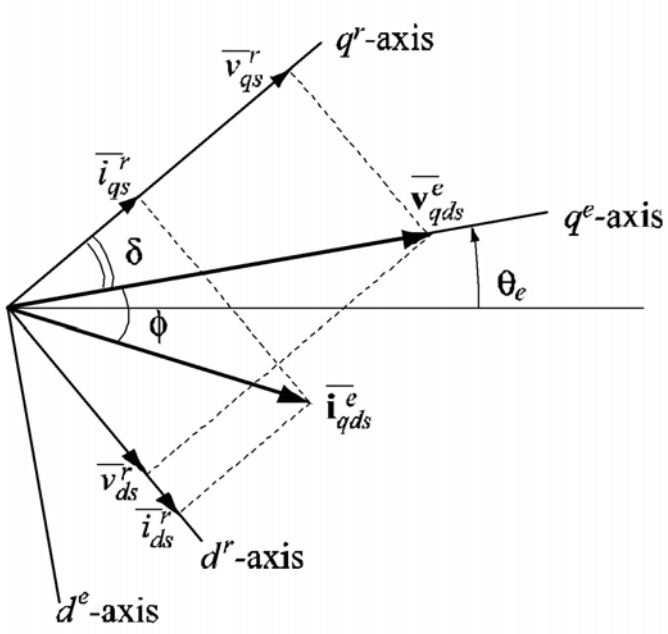

Figure 3: Relationship between the generator-rectifier variables in rotor and in synchronous reference frames.

If the generator is supplying real power, the rotor reference frame is leading the terminal voltages by the rotor angle δ. In Fig. 3 it is assumed that the fundamental component of the generator currents has a lagging power factor and the averaged current $\overline{i}^{e}_{qds}$ lags the voltage $\bar{\mathbf{v}}^{e}_{qds}$ by the angle ϕ.

The key point of parametric average value modeling presented here is to combine both rectifiers and relate the total averaged dc current $\overline{i}_{dc}$ to the currents $\overline{i}^{e}_{qds}$, and the final averaged output voltage $\bar{v}_{out}$ to the rectifier input voltages $\bar{\mathbf{v}}^{e}_{qds}$, respectively. We begin with the assumption that the system is implemented without the interphase transformer. In this case, the rectifier does not contain energy-storing components, and it is reasonable to approximate these relationships as

$$\left\|\bar{\mathbf{v}}^{e}_{qds}\right\| = \alpha \bar{v}_{dc} \tag{5}$$

$$\overline{i}_{dc} = \beta \left\|\overline{\mathbf{i}}^{e}_{qds}\right\| \tag{6}$$

where α and β are some algebraic functions of the loading conditions. In order to completely describe the rectifier, it is necessary to establish the angle between the vectors $\bar{\mathbf{v}}^{e}_{qds}$ and $\overline{i}^{e}_{qds}$. From Fig. 3, this angle can be expressed as

$$\phi = \arctan\left(\frac{\overline{i}^{r}_{ds}}{\overline{i}^{r}_{qs}}\right) - \delta. \tag{7}$$

Provided that functions (5)-(7) are available, the proposed average-value model is structured as shown in Fig. 4(a), wherein the generator is represented by a proper state model with stator currents as outputs and voltages as inputs. In this way, the generator can be readily modeled using classical approach based on $q-d$ Park's equivalent circuits [20] extended to the six phase case [22]. Alternatively, since the detailed model is already in VBR form that uses rotor reference frame transformations, it is straightforward to augment the model in Fig. 2 by removing the rectifier circuit and replacing it with an equivalent algebraic block.

This, in turn, suggests that the input and output of the rectifier AVM are $\bar{v}_{dc}$ and $\overline{i}_{dc}$, respectively. On the one hand, this condition is readily accommodated when there is no interphase transformer, in which case the capacitor voltage $v_{out} = v_{dc}$, and the filter capacitor C_f is modeled using a first-order state equation ($H_C(s) = 1/C_f s$) with v_{out} as a state variable, for example.

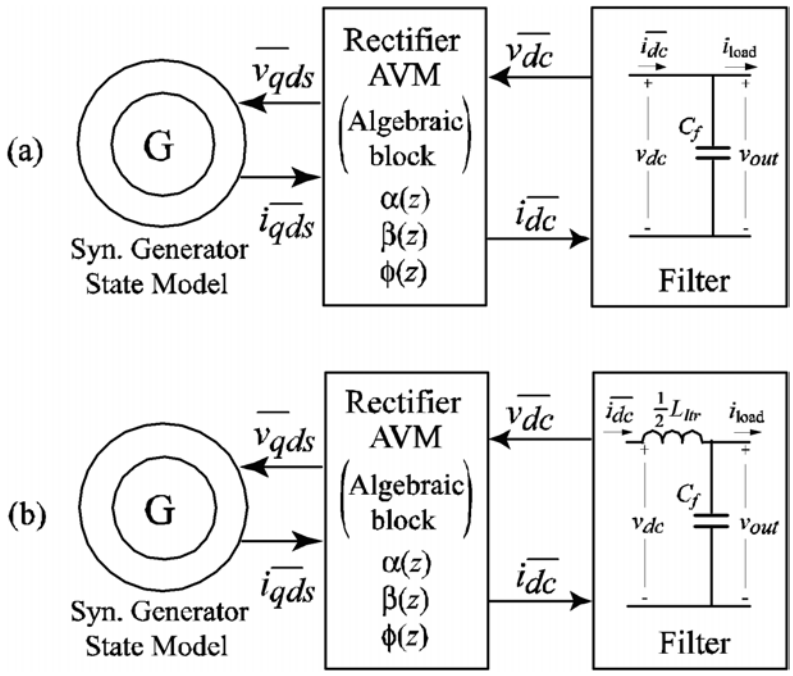

Figure 4: Average value modeling with the rectifier represented as an algebraic block; (a) system without interphase transformer; (b) system with interphase transformer which is represented by its leakage.

On the other hand, when the interphase transformer is present, its effects can be incorporated into the averaged model as shown in Fig. 4b. In the steady-state, the resistive voltage drop across the interphase transformer windings can be readily absorbed into $\alpha(\cdot)$ and $\beta(\cdot)$. However, the equivalent inductance of the transformer also impacts the output impedance, particularly in the range of higher frequencies. In order to account for this effect, the rectifier dc voltage is related to the capacitor output voltage in the frequency domain as

$$v_{dc} = v_{out} + H_{tr}(s)\, i_{dc}. \tag{8}$$

In order to avoid the numerical differentiation when implementing (8) in the time domain, $H_{tr}(s)$ must be properly chosen. Moreover, because of the way the interphase transformer windings are connected, the effect of mutual inductance cancels leaving only the leakage. Also, since the two rectifiers operate in parallel, the final equivalent inductance required in $H_{tr}(s)$ is one-half of the transformer leakage inductance. Therefore, in order to represent

the effective dynamics of the interphase transformer in the range up to the rectifier switching frequency, it is assumed that

$$H_{tr}(s) = \frac{0.5 L_{ltr} s}{\tau s + 1} \tag{9}$$

where τ is a time constant small enough so that its effect at the switching frequency is negligible (we used it to be 10^{-6}).

In general, the functions α, β, and ϕ are non-linear and depend on the system states which, in turn, depend upon the rectifier loading conditions. The loading conditions may be specified in terms of dynamic impedance, which can be conveniently defined as an operation point in terms of the state variables as

$$z = \frac{\bar{v}_{out}}{\left\| \overline{i}^{e}_{qds} \right\|}. \tag{10}$$

The selection of variables in (10) ensures availability of voltage and current from the respective detailed and averaged state models without introducing algebraic loops. It is extremely difficult to obtain expressions for $\alpha(z)$, $\beta(z)$, and $\phi(z)$ analytically. Instead, the approach taken here utilizes a detailed simulation to obtain several values of these functions numerically. In particular, more than one set of values is required in order to represent the slope of these functions at the operating point of interest.

The detailed model depicted in Fig. 2 has been used for computing α, β, and ϕ according to their definitions (5)-(7) and (10). Since the nominal load is assumed to be 12Ω, the values of these functions were determined numerically at the points slightly below and above the rated load. The resulting values for the four system configurations are summarized in Table 2. Although it may appear that the values of α, β, and ϕ do not change significantly with the loading conditions, it was found that accuracy up to four digit is required to match the detailed model well. The variables in (5)-(7) were obtained by averaging the respective currents and voltages in the steady-state over the rectifier switching interval.

Once these functions are available (as a look-up table with appropriate interpolation), the proposed average model is implemented according to Figs. 4 and 2. In particular, the impedance z is computed according to (10) and the functions α, β, and ϕ are evaluated for a given value of z. Based upon ϕ, the rotor angle is computed using

$$\delta = \arctan\left(i^{r}_{ds} / i^{r}_{qs}\right) - \phi(z). \tag{11}$$

The dc-link current is computed using

$$i_{dc} = \beta(z) \left\| \mathbf{i}^{r}_{qds} \right\|. \tag{12}$$

The generator voltages are expressed using the vector relationships depicted in Fig. 3 and (8) as

$$v_{qs}^{r} = \alpha\left(z\right) v_{dc} \cos\left(\delta\right) \tag{13}$$

$$v_{ds}^{r} = \alpha\left(z\right) v_{dc} \sin\left(\delta\right). \tag{14}$$

Thereafter, the difference $\mathbf{e}''_{qds} - \mathbf{v}_{qds}^{r}$ is passed to the transformation $[\mathbf{K}_{s}^{r}]^{-1}$ shown in Fig. 2.

System config.	Without interphase transformer		With interphase transformer	
	Neutrals disconnected (case 1)	Neutrals connected (case 2)	Neutrals disconnected (case 3)	Neutrals connected (case 4)
α	0.6170 / 0.6155	0.5503 / 0.5468	0.6175 / 0.6165	0.5756 / 0.5742
β	1.8157 / 1.8149	1.5785 / 1.5765	1.8157 / 1.8143	1.6768 / 1.6742
ϕ	0.1700 / 0.1555	0.2645 / 0.2445	0.1689 / 0.1468	0.2192 / 0.2186
z	19.970 / 23.592	17.363 / 20.499	19.970 / 23.570	18.451 / 20.754

Table 2: Rectifier parameters for the 11/13Ω load.

4 Computer studies

The detailed state model of the synchronous machine rectifier system described in Section II has been implemented in Matlab/Simulink as a masked CMEX S-function. The resulting detailed model was used as a benchmark in subsequent studies. The AVM depicted in Fig. 4 has also been implemented in Simulink using standard library blocks. In order to fully validate the averaged model against the detailed simulation, the respective models were compared in the frequency-domain. In all cases, a constant excitation of 502V and generator speed 1507 rad/sec was assumed. Because the average model only approaches the detailed model in terms of accuracy, the response produced by the detailed model is considered as a reference.

4.1 Operational modes

In cases 1 and 2, the interphase transformer was disconnected from the circuit and nodes 7, 8, and 12 were combined into a single node (see Fig. 2).

In order to demonstrate various operational modes of the system, the following time-domain study has been implemented using the detailed model with and without the interphase transformer. First, the system starts up with initial conditions closely corresponding to a steady-state operation with load resistance of 12Ω. At time $t = 0.01$sec, the generator neutrals are connected using the switch S branch 19. The computer generated response of the phase $as1$ voltage and current, and output dc voltage and current is depicted in Figs. 5-6. The corresponding operational modes that are determined by the sequence of the number of conducting diodes are summarized in Table 3. Similar computer studies have been verified against the hardware measurements in [15] which are not included here due to space limitations.

System configuration	Without interphase transformer		With interphase transformer	
	Neutrals disconnected (case 1)	Neutrals connected (case 2)	Neutrals disconnected (case 3)	Neutrals connected (case 4)
sequence of conducting diodes	4-6	3-5	4-6	4-5
number of topologies in a cycle	12	12	12	24

Table 3: Rectifier operational modes for the 12Ω load.

As noted in Figs. 5-6, when the generator neutrals are disconnected (cases 1 & 3), the voltage and current waveforms are almost identical. In cases 1 & 3, the upper and lower rectifiers essentially operate as two independent three-phase rectifiers connected in parallel and shifted by 60 degrees thus producing dc voltages with the same in-phase ripple. Since the dc voltages have in-phase ripple, the interphase transformer (case 3) does not produce the desired harmonic cancellation and has very little effect. This explains the fact that cases 1 and 3 have the same operational modes consisting of repeating sequence of 4 and 6 conducting diodes as summarized in Table 3. Also, since the rectifiers operate in parallel, the currents are equally divided between the two sets of stator windings. Therefore, each diode conducts only approximately one-half of the total load current during its conduction period as shown in Figs. 5-6 (for $t < 0.01$ sec.)

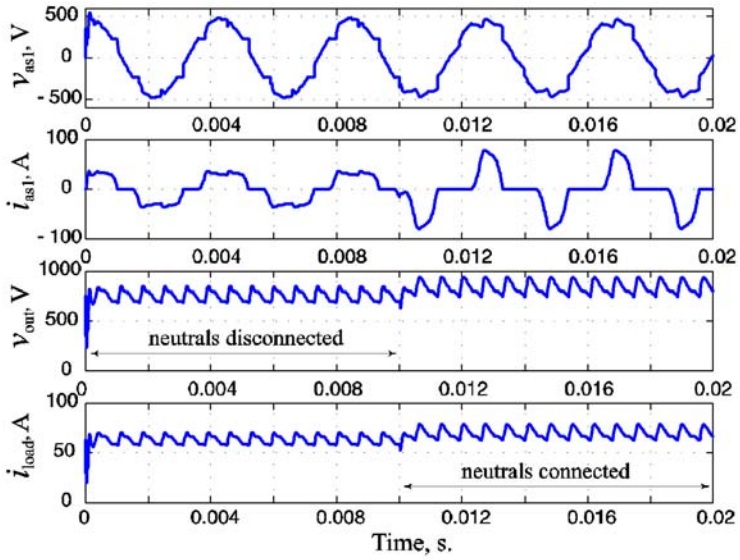

Figure 5: System operation without interphase transformer (cases 1 & 2).

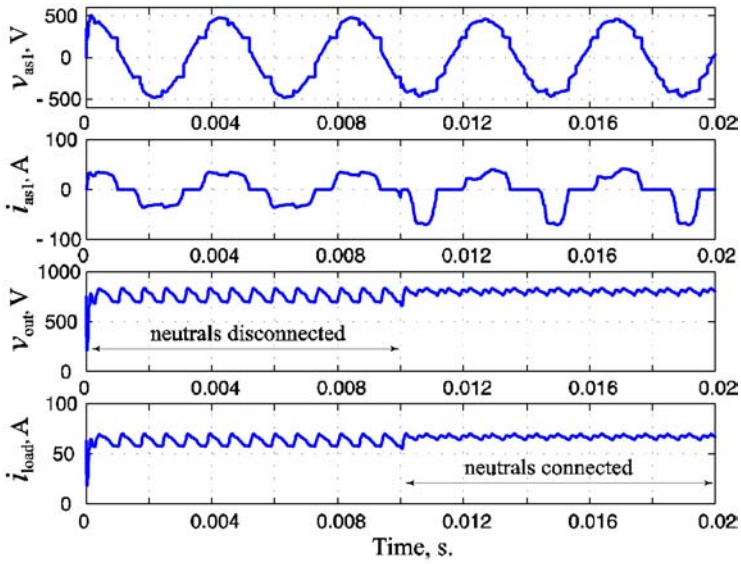

Figure 6: System operation with interphase transformer (cases 3 & 4).

The system performance changes significantly when the generator neutrals are connected to one another. Without the interphase transformer (case 2), the diode conduction interval is approximately one-half of that in cases 1 and 3. Additionally, each diode and stator winding conducts the peak load current for a part of the period. This can be observed by comparing the current waveforms in Fig. 5 before and after the generator neutrals were connected. As a result of that, the operating mode also changes and the number of conducting diodes decreases from 4-6 to 3-5 as shown in Table 3.

Interesting effects occur when the system operates with the interphase transformer (case 4). In particular, since the neutrals are connected to one another and the negative rails of both rectifiers are common, the load current can return through any of the six negative rail diodes. However, the positive rails are separate, resulting in the splitting of the load current between the two bridges. Also, because of the 60-degree shift of the stator windings, the voltage ripple produced by each bridge is out of phase. Therefore, the output dc voltage ripple corresponding to this circuit configuration is less than in other cases. However, as it can be observed in Fig. 6 (for $t > 0.01$ sec.), the ac currents are asymmetrical. Also, the overall number of topologies has increased from 12 to 24. More detailed analysis [15] can reveal that the diodes connected to the negative rail participate in only 5 out of 24 topologies, whereas the diodes connected to the positive rail participate in 9 of them.

4.2 Output impedance

Despite the fact that the functions α, β, and ϕ were computed under resistive load, the developed average value model should exhibit the same frequency-domain characteristics as the reference system (detailed model). Since the detailed model is discontinuous, the small-signal injection and subsequent frequency sweep method has been implemented in the same Simulink model and used to extract the required impedance information. The impedances are evaluated in the frequency range from 1 to 1000 Hz. Closer to the rectifier switching frequency the results become distorted due to the interaction of the injected signal with the rectifier switching, which requires more cycles in order to average and obtain an accurate point at a given single frequency. In general, the choice of frequencies close to and above the switching frequency has a limited use for the average model since the basic assumptions of averaging are no longer valid. The impedances are plotted in Figs. 7-10 for the four considered cases, respectively. On each figure, the impedance predicted by the detailed model is considered as a reference and is shown by "x" or "+".

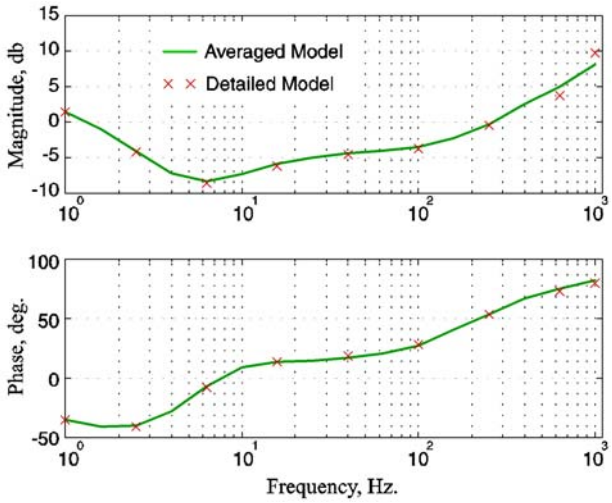

Figure 7: Output impedance predicted by the detailed simulation and the average value model for the systems without interphase transformer and generator neutrals disconnected (case 1).

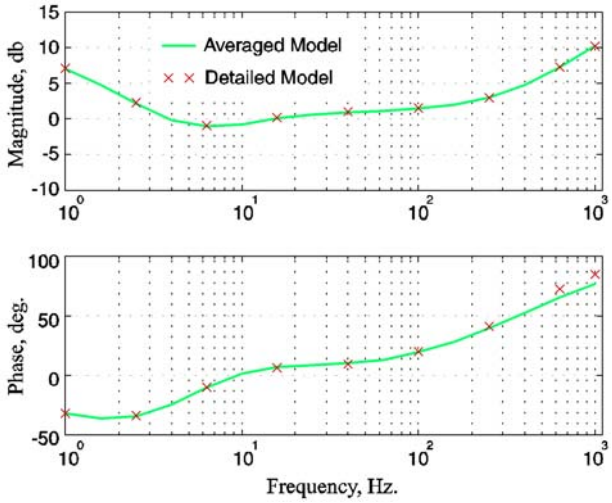

Figure 8: Output impedance predicted by the detailed simulation and the average value model for the systems without interphase transformer and generator neutrals connected (case 2).

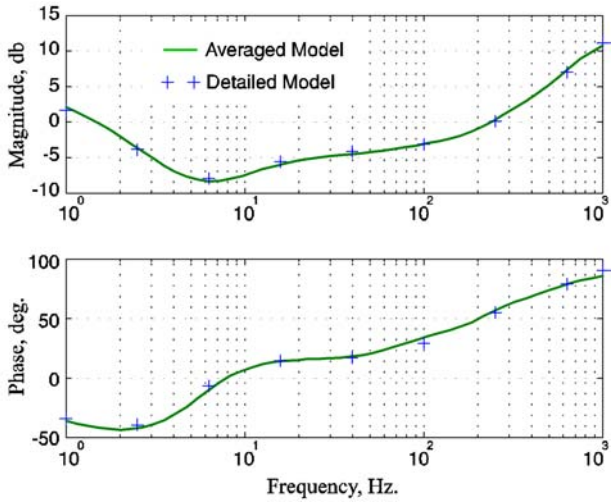

Figure 9: Output impedance predicted by the detailed simulation and the average value model for the systems with interphase transformer and generator neutrals disconnected (case 3).

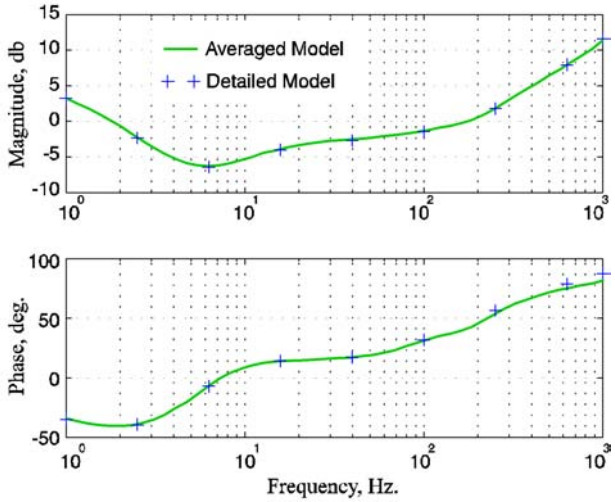

Figure 10: Output impedance predicted by the detailed simulation and the average value model for the systems with interphase transformer and generator neutrals connected (case 4).

The AVMs were also implemented with the rectifier parameters as summarized in Table 2. Since these models are continuous, the required output impedance can be extracted using linearization technique as well as the frequency sweep (both yielding identical results). The corresponding impedance curves are also plotted in Figs. 7-10 by solid lines. As can be seen in Figs. 7-10, the average model for each case matches the reference impedance almost exactly over the entire frequency range considered. As it was mentioned earlier, the slope of variables α, β, and ϕ captured in Table 2 was found to be an important factor. In particular, it has been found that, e.g., using constant values for α, β, and ϕ equivalent to their averages immediately leads to significant errors in impedance magnitude and phase, especially in 5-7 Hz range.

As it can be noted in Figs. 7 and 9, when the generator neutrals are disconnected (cases 1 & 3), the interphase transformer has almost no effect on the output impedance in the low frequency range, 1 – 100 Hz. However, its effect of increasing the impedance magnitude becomes more noticeable at higher frequencies. This difference can be observed by comparing Figs. 7 and 9 closer to 1 kHz range. As it can be seen in Fig. 9, the developed averaged model using (8)-(9) matches the high frequency range very well.

Connection of the generator neutrals changes the operating mode, diminishing the conduction intervals. This, in turn, leads to increase of the output impedance. In particular, without the interphase transformer (case 2), the diode conduction interval is reduced (one-half of that in cases 1 and 3), and each diode and stator winding conducts the entire load current for a part of the period. That is why the impedance magnitude shown in Fig. 8 is significantly higher than that in cases 1 and 3. Adding the interphase transformer (case 4) has yet another effect on the output impedance. In particular, as can be seen in Fig. 10, adding the interphase transformer has reduced (not increased!) the output impedance as compared with case 2 (Fig. 8). This reduction of the impedance is attributed to the change in operational mode (see Table 3), wherein the conduction interval of the diodes conducting positive current has increased (see Fig. 6, for $t > 0.01$ sec).

5 Conclusion

In this paper, an average value model of a six-phase synchronous generator-rectifier system with an interphase transformer has been developed using a parametric averaging approach. The possibility of connecting/disconnecting the generator neutrals, including/excluding the interphase transformer, etc.,

results in different operational modes that are difficult to establish analytically. This represents a big challenge for constructing appropriate average-value models and subsequent small-signal (impedance) characterization of the system. In the proposed method, the synchronous machine is implemented in a proper state model form, which can be VBR or classical *qd*-formulation. The functions defining relationship between the averaged dc-link variables and the generator currents and voltages viewed in the synchronous reference frame were implemented using linear approximations. The values of these functions were obtained numerically by running the detailed simulation in steady-state corresponding to distinct operating points around the operating point of interest. Four topological variations of the generator-rectifier system with distinct operational modes were considered and analyzed in time- and frequency- domain. An excellent agreement between the developed average value models and the detailed simulations was demonstrated for each considered case and operational mode.

This work was supported by grant from the Natural Science and Engineering Research Council of Canada.

References

[1] P. Huynh and B.H. Cho, IEEE Trans. on Circuits and Systems **45**, 377 (1998).

[2] S.D. Sudhoff, S.F. Glover, P.T. Lamm, D.H. Schmucker, D.E. Delisle, and S.P. Karatsinides, IEEE Trans. on Aerospace and Electronic Systems **36**, 965 (2000).

[3] M.B. Harris, A.W. Kelley, J.P. Rhode, and M.E. Baran, IEEE Applied Power Electronics Conference (APEC'94), vol.**2**, p.887 (1994).

[4] *Simulink: Dynamic System Simulation for Matlab*, Using Simulink. Version 5, Simulink LTI Viewer. (The MathWorks Inc., 2003).

[5] H.A. Peterson and P.C. Krause, IEEE Trans. on Power Apparatus and Systems **85**, 210 (1966).

[6] P.C. Krause and T.A. Lipo, IEEE Trans. on Power Apparatus and Systems **88**, 588 (1969).

[7] S.D. Sudhoff and O.Wasynczuk, IEEE Trans. on Energy Conversion **8**, 92 (1993).

[8] S.D. Sudhoff, IEEE Trans. on Energy Conversion **8**, 408 (1993).

[9] S.D. Sudhoff, K.A. Corzine, H.J. Hegner, and D.E. Delisle, IEEE Trans. on Energy Conversion **11**, 508 (1996).

[10] J.T. Alt, S.D. Sudhoff, and B.E. Ladd, IEEE Trans. on Energy Conversion **14**, 37 (1999).

[11] I. Jadric, D. Borojevic, and M. Jadric, IEEE Trans. on Power Electronics **15**, 303 (2000).

[12] J. Jatskevich, S.D. Pekarek, and A. Davoudi, In press, IEEE Trans. on Energy Conversion, 11 pages (2005).

[13] H.J. Hegner, P.C. Krause, O. Wasynczuk, E. Walters, and S. Pekarek, Proceedings of the 31st IECEC'96, vol. **3**, p.1792 (1996).

[14] W.L. Tucker, P.C. Krause, O. Wasynczuk, S.D. Pekarek, and E.A. Walters, Proceedings of the 31st IECEC'96, vol. **3**, p.1804 (1996).

[15] J. Jatskevich, O. Wasynczuk, S.D. Pekarek, E.A. Walters, C.E. Lucas, and P.T. Lamm, SAE Trans., Journal of Aerospace, Sect. 1, Set 3, p. 955 (2000).

[16] O. Wasynczuk and S.D. Sudhoff, IEEE Trans. on Power Systems **11**, 1951 (1996).

[17] J.R. Marti and K.W. Louie, IEEE Trans. on Power Systems **12**, 222 (1997).

[18] S.D. Pekarek, O. Wasynczuk, and H.J. Hegner, IEEE Trans. on Energy Conversion **13**, 42 (1998).

[19] S.D. Pekarek, and E.A. Walters, IEEE Trans. on Energy Conversion **4**, 1177 (1999).

[20] P.C. Krause, O. Wasynczuk, and S.D. Sudhoff, *Analysis of Electric Machinery and Drive Systems*, (IEEE Press, Wiley, 2002).

[21] C.M. Ong, *Dynamic Simulation of Electric Machinery: Using MATLAB/SIMULINK*, (Prentice Hall, 1997).

[22] R.F. Schiferl, and C.M. Ong, IEEE Trans. on Power Apparatus and Systems **102**, 2685 (1983).

[23] J. Jatskevich, O. Wasynczuk, C.E. Lucas, and E.A. Walters, Proc. 6th Int. Conf. on Computational Methods in Electrical Engineering and Electromagnetics (ELECTROCOMP'03), Split, Croatia, p.157 (2003).

[24] J. Jatskevich, and T. Aboul-Seoud, IEEE Int. Symp. on Circuits and Systems (ISCAS'04), Vancouver, Canada, paper PSEC-P2.4 (2004).